Journal of Petroleum Exploration and Production Technology (2024) 14:1071–1083
https://doi.org/10.1007/s13202-024-01754-2

ORIGINAL PAPER-PRODUCTION ENGINEERING

Evaluating the intake plugging effects on the electrical submersible pump (ESP) operating conditions using nodal analysis

Joseph Iranzi[1,2] · Jihoon Wang[3] · Youngsoo Lee[4] · Hanam Son[1]

Received: 2 August 2023 / Accepted: 12 January 2024 / Published online: 14 February 2024

Abstract

The intake plugging of an electrical submersible pump (ESP) has presented a formidable challenge to conventional ESP wells. Attention to cumulative solid deposition is essential since it intensifies the intake plugging severity and impedes ESP performance. We present a new approach to evaluate the ESP performance degradation during increased intake plugging severity. In particular, we employ the intake plugging factor, rate-derating factor, and affinity law to calculate the new ESP speed at different plugging conditions. We used Schlumberger PIPESIM software to perform nodal analysis of the newly calculated ESP speed. The result was validated using the actual field data and compared to the field cases that reported the intake plugging issue. The nodal analysis showed a steady maximum ESP head with zero rate derating at the shut-in point. The intake plugging factor caused a significant reduction in the ESP operating rate and increased pump intake pressure and annulus liquid level. Based on the existing intake plugging field data, we established the quantitative standard for the normal and abnormal intake plugging factor range. The observed results agreed with the field downhole data recorded during the intake plugging problem. We identified that regulating the ESP speed to the reduced operating rate could minimize unexpected pump stoppage. It is also possible to carefully monitor the intake plugging problem by combining the annulus liquid level, the signature of pump intake pressure, and a deadhead test.

Keywords Electrical submersible pump (ESP) · Intake plugging factor · Nodal analysis · Rate-derating factor

List of symbols

a, b, c, d, e, f	ESP head coefficients
BHP	Bottomhole pressure (psia)
dP	Pump differential pressure (psia)
DP_{fr}	Tubing friction pressure loss (psia)
$grad_{FT}$	Flowing tube gradient (psia/ft)
$grad_L$	Hydraulic pressure gradient of the produced fluid (psia/ft)
H	ESP developed head (ft)
H-Q	Head-rate curve
L_{dyn}	Annulus dynamic liquid level (ft)
L_{set}	Pump setting depth (ft)
n	Pump stage number
P_d	Pump discharge pressure (psia)
PIP	Pump intake pressure (psia)
P_{wh}	Wellhead pressure (psia)
q	Operating well production rate (stb/day)
q_o	ESP normal operating rate (stb/day)
q_x	ESP operating rate after a certain percentage of plugging (stb/day)
R_f	Rate-derating factor

Greek symbols

ρ_L	Fluid density (ppg or 7.5*lb/ft^3)
ω	ESP rotational speed (Hz)

Acronyms

AI	Artificial intelligence
AL	Artificial lift
AOF	Absolute open flow
BHP	Bottomhole pressure
ESP	Electrical submersible pump
IPF	Intake plugging factor
IPR	Inflow performance relationship

✉ Hanam Son
hason@pknu.ac.kr

[1] Department of Energy Resources Engineering, Pukyong National University, 45 Yongso-Ro, Nam-Gu, Busan 48513, Korea

[2] Department of Mining, University of Rwanda, 3900 Kigali, Rwanda

[3] Department of Earth Resources and Environmental Engineering, Hanyang University, Seoul 04763, Korea

[4] Department of Mineral Resources and Energy Engineering, Chonbuk National University, Jeonju 54896, Korea

PIP	Pump intake pressure
PVT	Pressure, volume, and temperature
TPR	Tubing performance relationship
VFD	Variable frequency drive
VSD	Variable speed drive

Introduction

Recently, an electrical submersible pump (ESP) occupies 20% of all artificial lift (AL) pumps used in global oil production. ESP is a cost-effective artificial lift method for high and moderate-fluid rate reservoirs; however, it is inefficient when operated in a solid deposition environment (Fakher et al. 2021; Takacs 2018). The solids deposition results from the precipitation of high molecular weight compounds and solution metals associated with produced fluid, which makes organic and inorganic solids precipitate, respectively (Alizadeh et al. 2011; Ramones et al. 2015; Vazirian et al. 2016; Zendehboudi et al. 2014). Like the other production problems (e.g., gas locking, (Iranzi et al. 2022)), solid deposition presented a formidable challenge to conventional ESP technologies because it leads to semi or complete blockage of the ESP downhole equipment.

The intake screen is alternatively employed at the ESP intake point to handle solid problems in the ESP well. Unfortunately, its small opening creates a higher volume rate, resulting in fluid phase segregation and intensifying the pressure drop at the ESP intake point. Also, most ESPs operated near the pump-off condition to improve the drawdown; at this point, the pump intake pressure is approximately equal to the bubble point pressure, which accelerates the organic and inorganic solid deposits around the pump intake screen, inducing cumulative solid deposition (Chouparova et al. 2004; Correra et al. 2016; Denney 2000; Mohammadzadeh et al. 2018). Typically, a cumulative solid deposition increases pressure drops, and the higher pressure drops amplify the hydraulic losses, significantly affecting the pump head, resulting in the pump shutdown and creating an additional production problem. Hence, a suitable approach is needed to monitor ESP well in a solid deposition environment since the intake screen cannot solely provide an effective solution.

Researchers developed various ESP monitoring perspectives to avoid the submersible motor starting and stopping several times daily. Dowling and Lemus (2023) demonstrated the application of pressure derivatives to evaluate the ESP failure, resulting from intake plugging. Since the pressure derivative calculates the flow rate in the tubing and annulus, it can detect events like no-flow conditions induced by inflow plugging. Still, applying this approach requires more attention since it can compromise the ESP diagnosis when multiple issues coincide. Lastramelo et al. (2023) presented a combination of machine learning and physics-based damage modeling to predict ESP failure, such as intake plugging. The proposed approach needs accurate input data for the normal range and abnormal range to indicate the ESP abnormalities based on the ESP input parameters deviation, which limits the applicability of this system to the new ESP well where these data are unavailable.

Moreover, Agrawal et al. (2019) combined time-lapse analysis, ESP alarm system parameters, variable frequency drive (VFD) horsepower, deadhead, and multi-choke test data to assess ESP well failure spawned by polymer flooding. Their study provided an ESP well diagnostic approach to differentiate the polymer intake plugging, gas lock, and leakage-related failure. Still, it is complex to apply to the new ESP well design. Adesanwo et al. (2017) developed a decision support system to manage the ESP well condition to avoid unexpected failure. The system uses real-time data signals to forecast ESP failure instances. However, this system needs the input data of normal and abnormal conditions, and it cannot be generalized to a new ESP well. Awaid et al. (2014) generated a pattern recognition analysis that uses real-time data from the ESP well to diagnose ESP failure conditions (including ESP intake plugging). They strictly focused on retrospective monitoring, which is complex to apply to the new ESP well design. Bermudez et al. (2014) employed probabilistic (Fuzzy) logic to process ESP diagnosis. It combines the AI tool that calculates a slope for real-time data signal trends, comparing them with pre-established rules. Nevertheless, this approach needs accurate pre-existing data and limits its application in new ESP systems.

The previously developed approaches for monitoring ESP well only provided a retrospective monitoring solution for the intake plugging failure. However, the intake plugging-related failure can be monitored in advance with an early warning approach before ESP installation and prevents ESP failure before it happens. Our previous paper (Iranzi et al. 2022) employed the nodal analysis to detect the onset of abnormal ESP operation conveyed by the rise in free gas in the pump. We performed the nodal analysis at both the intake and discharge point of the pump using the differential pump pressures calculated at various gas volume fractions. The effects of gas intake fraction variation were reflected through the simultaneous analysis of pump intake and discharge pressure and disclosed the ESP failure. Accordingly, nodal analysis proved to be a monitoring tool for future ESP wells by setting the normal operating range based on the natural operating condition and providing a proactive monitoring approach before the ESP deployment.

This study adopted the nodal analysis approach to evaluate the ESP operation during the cumulative intake plugging conditions to optimize the ESP operating mode in the solid deposition environment. The new approach introduced the intake plugging factor (IPF) to assess the ESP operating

conditions during the cumulative intake plugging. Based on the existing reported intake plugging field cases, we established the quantitative standard for normal and abnormal IPF operation ranges. We utilized Schlumberger PIPESIM software to predict ESP operating conditions at that IPF range, which reflects the ESP well operation under cumulative plugging. The new concept monitors the intake plugging problem by combining the annulus liquid level, pump intake pressure signature, and a deadhead test. The work is novel in that we evaluated the ESP performance degradation imparted by different intake plugging factor conditions; we evaluated the allowable intake plugging operation range before the ESP shutdown. The proposed approach can significantly reduce ESP failure since it can be compatible with new ESP wells and provide a proactive monitoring plan before ESP deployment based on the ESP natural well conditions.

Materials and methods

Effect of intake plugging on the ESP performance

The intake plugging has a detrimental effect on the ESP performance since it increases the head pump loss. Figure 1a shows different head losses associated with the ESP system, the hydraulic loss being among them, and it is associated with intake plugging. Divine et al. (1993) stated that intake plugging severity increases hydraulic losses. The vertical section of the pump head (H-Q) curve moves progressively to the left side of the pump, indicating performance degradation (Fig. 1b). Also, the experimental test of the ESP performance curve during the intake plugging has shown that the ESP head curve shifted to the left side until it became vertical at a constant production rate (Fig. 1c&d). As a result, during severe plugging, ESP loses its lift power, and the ESP-assisted well operates as a natural oil well until the zero production rate for a full blocked intake(Agrawal et al. 2019).

Rate-derating factor calculation

The rate derating is the change in the ESP operating rate due to the hydraulic loss intensity. We examined the hydraulic loss effects from the generated pump head curve (H-Q curve), which is augmented from the shut-in point (zero rate) to the absolute open flow (AOF) (maximum rates) (Agrawal et al. 2019). Figure 2a depicts the rate-derating effects on the ESP performance curve, which is relatively associated with hydraulic losses. Usually, the system curve is unaffected by the hydraulic losses, and it was kept constant during the intake plugging analysis. The only effects considered are the variation of the ESP performance curve during intake plugging and their

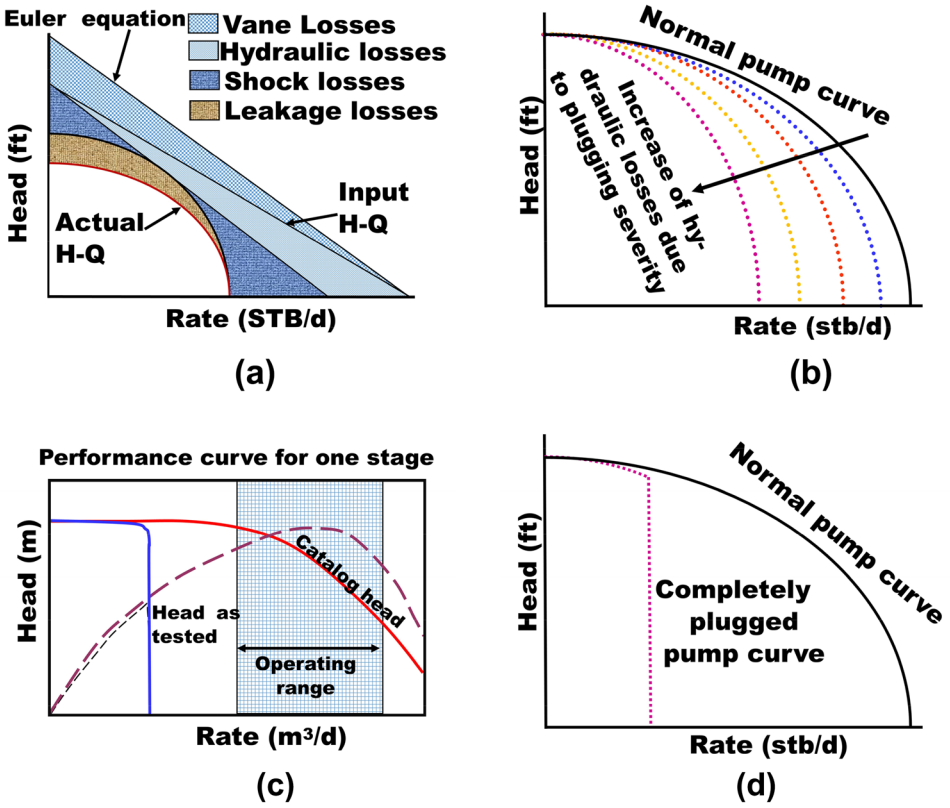

Fig. 1 Typical head losses in the ESP-assisted well. **a** Significant losses in the centrifugal pump. **b** Effect of the hydraulic losses to the ESP H-Q curve. **c** Test curve for intake plugged pump modified after Divine et al. (1993), **d** Pump head (H-Q) curve at the severe plugging condition modified after Agrawal et al. (2019)

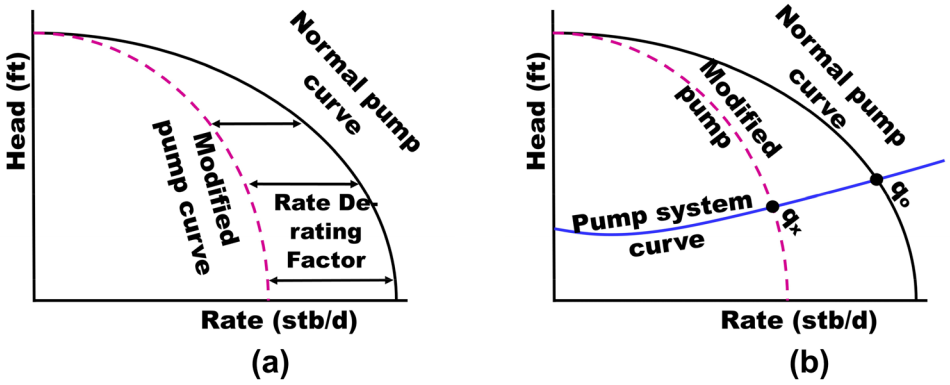

Fig. 2 **a** Rate-derating effect on the ESP head curve (H-Q). **b** Intake plugging affects the ESP operating rate modified after Agrawal et al. (2019)

corresponding effects on the ESP head and operating production rate (rate derating) (Fig. 2b).

The intake plugging severity was quantitatively analyzed using a newly proposed concept (intake plugging factor, IPF), which defines the percentage of the intake screen area filled with solids (e.g., for a half-plugged intake screen, the IPF is assigned to 0.5). Figure 3 highlights the severity of the ESP intake screen, which was considered to quantify the IPF. This study assumed the IPF to vary from 0 to 1 (0 indicates the intake condition before solids plugging, and 1 is the wholly plugged screen).

As shown in Fig. 2b, we assumed that intake plugging reduced the normal operating point from q_o to q_x (q_x, represents ESP operating rate after a certain percentage of plugging varies with IPF), correlated using a newly generated Eq. 1. A rate-derating factor (R_f) was computed from the ratio of the operating rate at the normal condition (q_o) to the operating rate at a specific plugging condition (q_x) as shown in a newly generated Eq. 2.

$$q_x = (1 - \mathrm{IPF}) q_o \tag{1}$$

$$R_f = \frac{q_o}{q_x} = \frac{1}{(1 - \mathrm{IPF})} \tag{2}$$

Simulation of nodal analysis for intake plugging

Calculating new ESP operating speed during plugging conditions

It is common for most ESP systems to have installed variable speed drives (VSD). The primary function of the VSD is to vary the ESP operating speed to increase the operating range (Wilson and Liu 1985) or adjust the ESP speed if the production rate is less than expected (Alcock 1981). The VSD reduces the ESP speed to avoid the motor burning or underloading trip, shutting down the ESP motor. Since the intake plugging reduces the operating rate, we used the affinity law to evaluate the change in the ESP speed according to the reduced production rate. The affinity laws state that for every point of a pump performance curve, the rate varies linearly with speed, Eq. 3; the head varies as the square of the speed, Eq. 4 (Powers 1987). The affinity law can compute the rotating equipment output parameters (e.g., centrifugal pumps). Then, we calculated a new ESP parameter from the known ESP initial parameters (such as developed head, operating speed, rate, and power). Subscript 1 indicates the known parameters, and 2 shows unknown parameters (Xian et al. 2014).

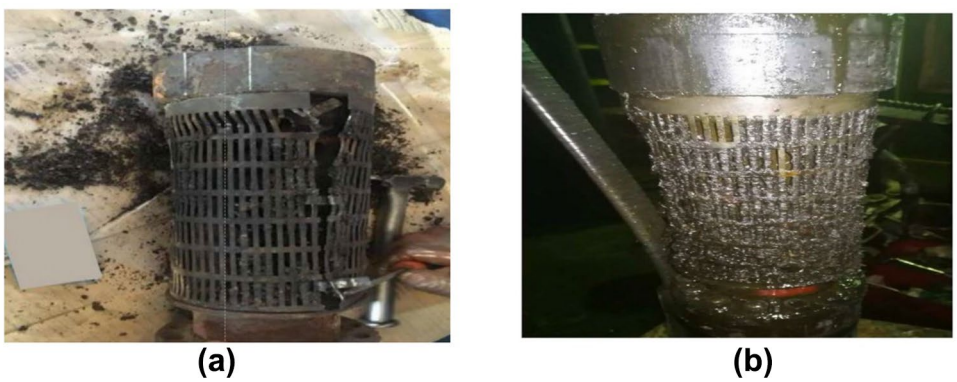

Fig. 3 A field example of the intake plugging severity. **a** A partially plugged intake screen, and **b** a wholly plugged screen modified from Abdelazim et al. (2022)

$$\frac{q_1}{q_2}=\frac{\omega_1}{\omega_2} \tag{3}$$

$$\frac{H_1}{H_2}=\left(\frac{\omega_1}{\omega_2}\right)^2 \tag{4}$$

We employed the affinity law to generate a new equation (Eq. 5) relating the intake plugging factor and ESP speed. Using Eq. 5, we computed the new parameters of the plugged pump according to the IPF. For instance, during the normal conditions, ESP was operating at the production rate of q_o with a rated speed (ω_o); then, due to a plugging, the production rate fell to production rate (q_x). After that, we performed nodal analysis using a newly generated operating speed (ω_x).

$$\omega_x = (1 - \mathrm{IPF})\,\omega_o \tag{5}$$

ESP intake plugging monitoring using nodal analysis

In principle, the nodal analysis can be employed in oil and gas production optimization, pinpointing the problems and contributing to the AL sizing. The point of interest in the production system acts as a node, an intersection point of the tubing performance relationship (TPR) and the inflow performance relationship (IPR) curves (Iranzi et al. 2022). In this study, the ESP intake node is the nodal analysis point to analyze the intake plugging. The TPR and IPR curves are governed by Eq. 6 and Eq. 7, respectively.

Inflow equation (IPR curve):

$$\mathrm{IPR} = \mathrm{PIP} \tag{6}$$

Outflow equation (TPR curve):

$$\mathrm{TPR} - \mathrm{ESP} = \mathrm{PIP} \tag{7}$$

Based on the field data that reported the intake plugging, we established the normal operation range (threshold operation range) and abnormal onset (ESP shutdown). For example, the severe ESP intake plugging in the Flanagan "B" oil well decreased the ESP operating speed from 55 Hz (a normal design ESP operating speed) to 0 Hz (at the fully plugged ESP intake, no fluid entering the pump) (Oyewole 2005). Awaid et al. (2014) reported that ESP speed drops to zero during the intake plugging when the ESP operating point moves to zero. Notably, the reason for the ESP speed dropping to zero is associated with a fully plugged intake, implying that the fluid is not entering the pump. It is imperative that the intake plugging should be monitored to avoid that disastrous condition (zero flow). As a result, we suggested that the cumulative plugging should be monitored in reference to the natural oil well condition by setting the ESP speed to turn the ESP operating point to the natural oil well condition. Implying that the ESP operated under the normal operation range when the production rate was higher than the natural oil well production rate. Conversely, the ESP operated in the abnormal condition when its operating production rate was equal to or less than the natural flowing condition. In detail, below are the steps for setting up the normal operating range according to the IPF:

Step 1 (Nodal analysis in the absence of the ESP): The nodal analysis was conducted under the natural flow condition before installing the ESP. From the nodal analysis, we estimated the production rate (q_1) and bottomhole pressure (BHP) (Fig. 4).

Step 2 (Nodal analysis in the presence of the ESP): After installing the ESP, we proceeded with the nodal analysis at the intake node; we recorded the operating ESP PIP (PIP_1), and production rate (q_2), representing the ESP operation at design condition (Fig. 5).

Step 3 (Calculating the ESP abnormal onset): We employed the affinity law to calculate the ESP speed corresponding to the natural well production rate obtained in step (1) using Eq. 3. We recorded the operating ESP PIP at the severe intake plugging (PIP_2), and production rate (q_3) (Fig. 6).

Step 4 (ESP abnormal IPF onset): We calculated the variation of the IFT with ESP speed using Eq. 5, and the

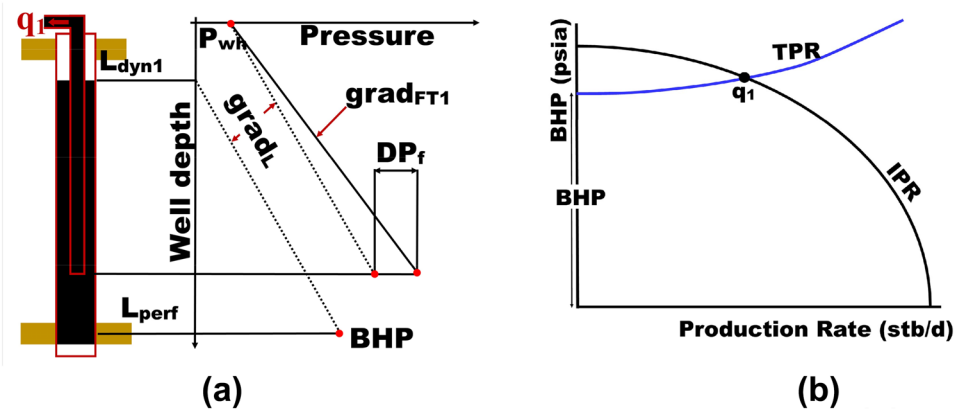

Fig. 4 Natural oil well-operating condition **a** pressure distribution **b** nodal analysis operating point. We assumed the oil well operated under natural conditions with a lower production rate (q_1) and high BHP, which correspond to the annulus liquid levels (L_{dyn1})

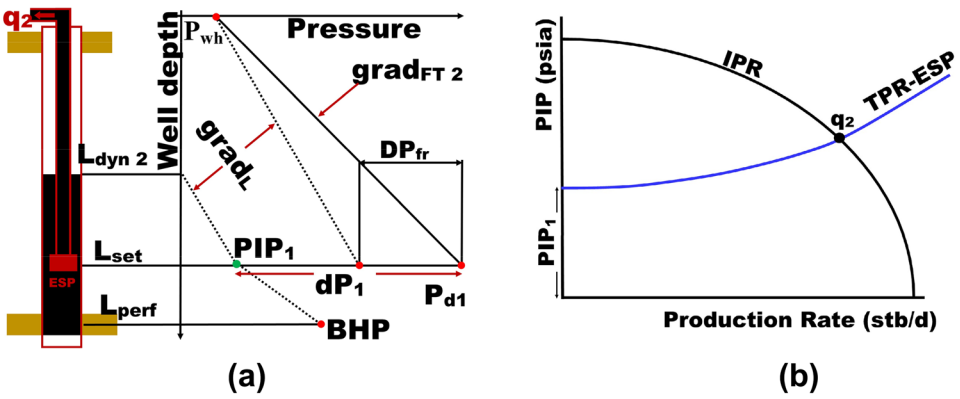

Fig. 5 ESP-assisted well operating condition (at ESP design condition) **a** pressure distribution **b** nodal analysis operating point. We assumed that the ESP installation would increase the production rate from q_1 to q_2, which lowers BHP to the PIP_1 and annulus liquid level from L_{dyn1} to L_{dyn2}

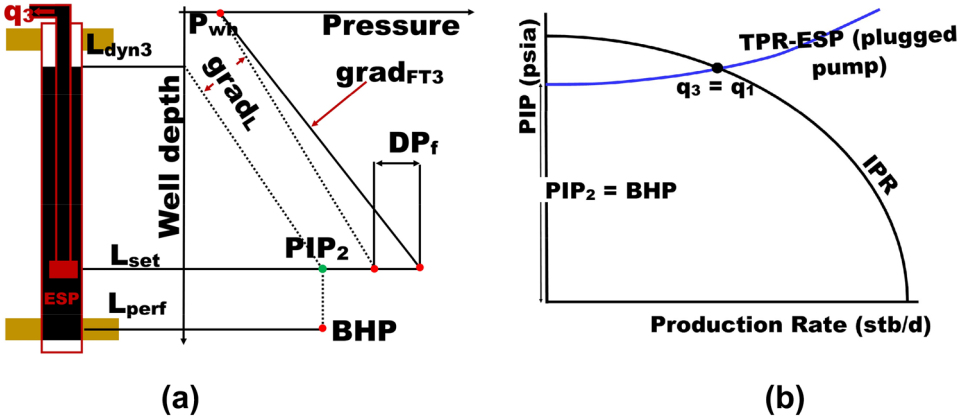

Fig. 6 ESP-assisted well operating condition during the severe intake plugging. **a** Pressure distribution **b** Nodal analysis operating point. Due to severe plugging that reduced the ESP performance, we assumed that the oil well production rate would be reduced from q_2 to q_3, increasing both PIP and L_{dyn} from PIP_1 to PIP_2 and L_{dyn2} to L_{dyn3}, respectively. The ESP performance is progressively decreasing, and the ESP well operating parameters will be affected until the ESP-assisted well is operating at the natural flow conditions (e.g., $q_3 = q_1$, $L_{dyn3} = L_{dyn1}$, and $PIP_1 = PIP_2$) at the severe plugging

ESP abnormal onset was evaluated where the ESP operating point coincides with the natural operating point.

Step 5 (Estimating the variation of the annulus liquid level (L_{dyn})): We employed the PIP obtained from the nodal analysis at different IPFs to compute the corresponding L_{dyn} using Eq. 8 and 9 (Takacs 2011).

$$L_{dyn} = L_{set} - \frac{PIP}{grad_L} \tag{8}$$

$$grad_L = 0.052\rho_L \tag{9}$$

Based on the above concept, we formulated the monitoring aspect to ESP-assisted well exhibiting the cumulative intake plugging. The proposed monitoring aspect combines PIP, BHP, operating production rate, and liquid level dynamic data to delineate the intake plugging issue (Table 1).

Table 1 ESP monitoring scheme during the cumulative intake plugging

ESP operating condition	Monitoring parameter
Permissible operation range	$q_2 > q_1$, $PIP_2 < BHP$ and $Ldyn < L_{dyn1}$
Abnormal operation range	$q_2 \leq q_1$, $PIP_2 \geq BHP$ and $L_{dyn} \geq L_{dyn1}$

Calculating the ESP performance variation during intake plugging

The ESP performance can be measured based on the production capacity of the pump, such as the head generated at the rated speed. As mentioned previously, intake plugging affects ESP performance, which consequently decrease rate to a certain amount. The new performance of the plugged pump was calculated using the rate-derating factor. The centrifugal pump

(e.g., ESP) standard performance curve (indicates the relationship between the pump head and the flow rate) was used to plot the head-flow rate curve after modifying Eq. 10 (Dholkawala et al. 2012).

$$H = \left(aq_o^5 + bq_o^4 + cq_o^3 + dq_o^2 + eq_o + f\right) \times n\left(\frac{\omega_o}{60}\right) \quad (10)$$

We employed Eq. 6 and 7 to generate the ESP performance curve. In detail,

Step 1: We generated the TPR and (TPR—ESP) curves using Schlumberger PIPESIM software by the ESP intake as a node (Fig. 7a).

Step 2: We subtracted (the TPR—ESP) curve from the TPR curve (Fig. 7b) to generate the ESP performance curve (dp_{pump} vs. production rate, Fig. 7c).

Step 3: We employed Eq. 11 to covert dp_{pump} obtained from step 2 into pump head (H), as shown in Fig. 7d. After that, we obtained the required ESP head factors (in Eq. 10 from Fig. 7d fitting equation). The head factors depend on the design operating speed, number of stages, and fluid properties, and it can vary depending on the pump selected, which permits adaptability to different well conditions.

$$H = \frac{dp_{pump}}{grad_L} \quad (11)$$

Example of scenario for methodology validation

We used the oil well data from the Delaware Basin to validate the proposed methodology. Using the modified ESP speed due to the intake plugging, we conducted the nodal analysis using the Schlumberger PIPESIM software (version 2017.01) to investigate the ESP operating point before and after plugging. Table 2 summarizes the input data for the example well. Firstly, we used the field oil well data to build and calibrate a well model using the field production

Table 2 Field example oil well data

Parameter	
Reservoir pressure (psia)	3378.93
Reservoir temperature (*F*)	206
Pay zone thickness (ft)	68
The horizontal distance (ft)	3901
Water cut (%)	92.9
Gas oil ratio (SCF/STB)	2218
Gas SG	0.65
API	42.98
Well-measured depth (ft)	12,216
Tubing measured depth (ft)	7021
Tubing ID (in)	2.785
Oil production rate (STB/d)	430

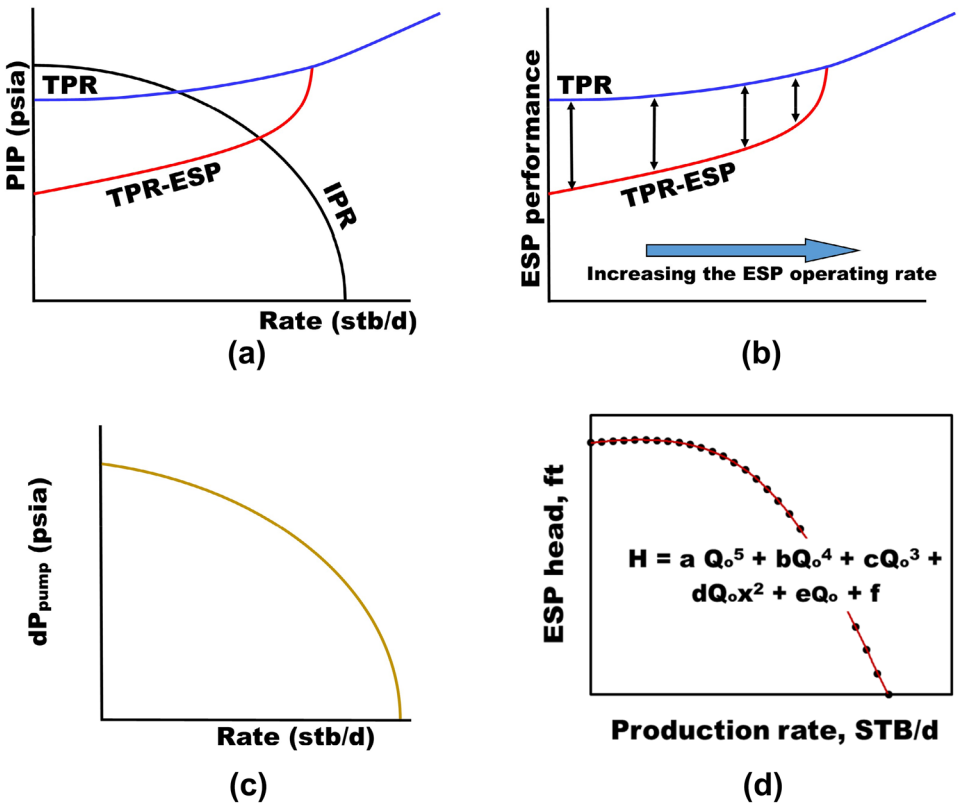

Fig. 7 ESP performance calculation. **a** *Step* 1: Nodal analysis plot at the ESP intake (TPR and TPR—ESP curve). **b** *Step* 2: Generating ESP performance curve (governed by the differential pressure). **c** Pump differential pressure variation with the production rate (obtained after subtracting the TRP-ESP curve from TPR curve), and **d** *Step* 3: ESP head curve versus production rate and ESP head factor calculation. TPR: Tubing performance relationship curve without ESP, and TPR—ESP: Tubing performance relationship curve with ESP

data. We adopted the Babu&Odeh pseudo-steady equation and Hagedorn & Brown correlation to build IPR and TPR curves, respectively (Beggs and Brill 1973; Babu and Odeh 1989; Hagedorn and Brown 1965; Manshad et al. 2019). We subsequently used the calculated operating speed at various IPFs and performed nodal analysis to evaluate the new ESP working condition. The nodal analysis generated the operating PIP, and we employed them to calculate the corresponding annulus liquid level.

To generalize the proposed methodology, even in the oil well extreme conditions, we tested it under different oil well conditions: (1) the multiphase conditions when GOR = 2218 SCF/STB and water = 92.9% (actual well data), (2) under the single-phase phase conditions when GOR = 100 SCF/STB and water = 0 (extrapolated data).

Results and discussion

Results of nodal analysis simulation

A detrimental effect of cumulative intake plugging on the ESP performance was evaluated using nodal analysis at the ESP intake point (nodal point placed at the ESP intake screen). During the nodal analysis, an intersection of the TPR-ESP and IPR curve yielded the operating PIP and production rate when the IPF increases. Figure 8a shows the nodal analysis of IPF variation for the multiphase condition; in this case, the ESP operating point intersects the natural well operating point when IPF ≥ 0.6, corresponding to the ESP operating speed of 24 Hz. Also, the ESP operating point intersects the natural oil well for an IPF ≥ 0.55, corresponding to the ESP speed of 27 Hz in single-phase flow (Fig. 8b).

In principle, the intersection of the ESP operating point and natural well operating point indicates the onset of the abnormal ESP conditions because, at this point, ESP is not contributing to the fluid lifting (ESP shutdown case). Also, the observed difference in the onset of an abnormal ESP operation for prescribed cases (multiphase vs. single-phase flow) indicates a significant effect of the produced fluid properties on the ESP performance. Iranzi et al. (2022) reported that during the multiphase flow, the fluid produced is lighter (e.g., gas content lowers the fluid density) than in single-phase flow and requires less energy than denser fluid. Since the intake plugging reduces the ESP performance, the onset of an ESP abnormal operation is turned on at a lower IPF (0.55) in a single-phase well compared to the IPF of 0.6 observed in the multiphase flow.

In addition, the simulation result shows that the ESP operating point (the intersection of the TPR-ESP and IPR curve) changes as the IPF increases; this increases the operating PIP and reduces the operating production rate. The TPR-ESP curve showed a typical upward movement in response to the increased PIP and production rate reduction. Iranzi et al. (2022) demonstrated that the upward movement of the TPR-ESP curve indicates the ESP performance degradation imparted from a detrimental increase of free gas in the ESP well, which confirmed similar findings when the IPF increased. Also, we noticed a leftward movement of the ESP operating point (intersection between the TPR-ESP curve and IPR curve) when the IPF rises, reflecting the ESP performance degradation. Bruijnen (2016) reported that when the ESP loses its lifting capacity, the increased PIP and reduced operating production are a signature of ESP performance degradation. Also, Pagan and Waltrich (2016), Lea and Nickens (2004), and Yadua et al. (2020) described the leftward movement of the ESP operating point as a signature of ESP operation instability during the severe increase of the free gas at the ESP intake point. The observed result from the nodal analysis during the increases in IPF agrees with the previous findings of the other parameters that compromise the ESP performance.

The results can be further interpreted over two categories based on the ESP operating point variation when the IPF increases.

Category I: ESP normal operation: The ESP operating point (intersection of TPR-ESP curve and IPR curve) stabilized below the natural flow operation point. At this

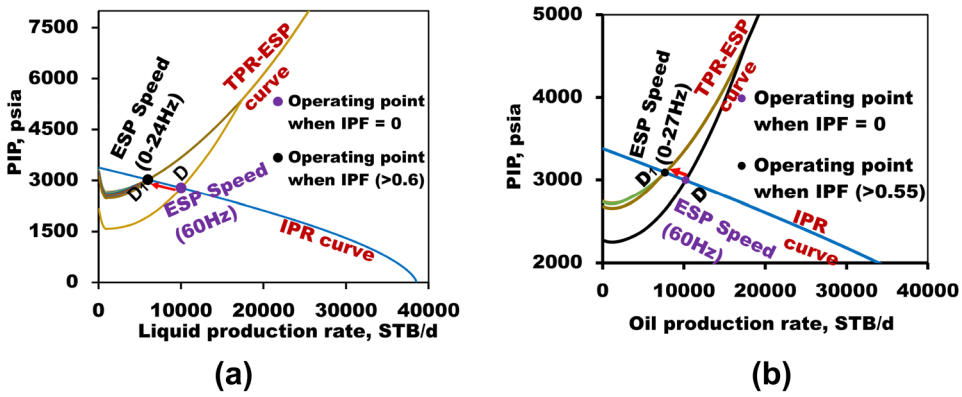

Fig. 8 The nodal analysis reflects decreasing the ESP speed on the ESP well-operating condition during the intake plugging. **a** Multiphase condition (GOR = 2218 SCF/STB and water = 92.9%) and **b** Single-phase condition (GOR = 100 SCF/STB and water = 0)

point, the recorded operating PIP is lower than the actual well BHP, which indicates that the ESP is still contributing to lowering the well BHP regardless of the intake plugging condition. For example, the ESP operating point remains below the natural well operating point until the IPFs of 0.6 and 0.55 are attained for multiphase and single-phase flows, respectively.

Category II: ESP shutdown condition: In this case, the ESP operating point coincided with the natural well operation point (e.g., the recorded operating PIP is equal to the actual well BHP), which indicates ESP is not contributing to the fluid lifting, its operating speed is significantly lower than the required speed to lower the well BHP. For example, from the IPF of 0.6 and 0.55 (multiphase and single-phase flows, respectively), their corresponding speeds no longer provide the required energy to lower the actual well BHP.

Variation of pump intake pressure and annulus liquid level

Generally, the PIP is widely employed to remark unanticipated changes below the ESP, and the annulus liquid level features a sudden variation of the casing fluid condition (Awaid et al. 2014). Since these features are analogous to the change anticipated from the intake plugging issues, it is requisite to understand that PIP and annulus liquid levels tide according to the IPF conditions. In both cases (multiphase and single-phase flow), a remarkable increase in the operating PIP and annulus liquid level was observed when IPF increased (Fig. 9). The increased tides of these parameters flash the ESP performance degradation, resulting from the intensified hydraulic losses conveyed from the progressive solid deposition. Likewise, the nodal analysis conducted on the IPF below 0.6 (Fig. 9a) and 0.55 (Fig. 9b) for multiphase and single-phase, respectively, noticed a steady PIP and annulus liquid levels trend. These results infer that the ESP no longer provided a required differential pressure to lower the actual well BHP and agreed with different field cases that exhibited intake plugging issues. For example, the ESP well swapped to the natural flow when half of the ESP intake screen plugs with solids in the Flanagan oil field. The recorded PIP was similar to the BHP observed when the ESP shutdown (Oyewole 2005).

Variation of ESP performance during the intake plugging

A deadhead test has been reported as a critical parameter to differentiate the solid deposition-related ESP failures (e.g., leakage) from the intake plugging. It indicates whether an ESP head reduction is due to hydraulic loss (intake plugging) or related to the ESP failure. During the test, ESP runs at its normal operating speed with zero surface flow rate (shut-in point) and records the ESP head variation at no flow. If any prominent change to the ESP head is detected at the no-flow condition, the intake plugging is not the cradle of ESP failure; otherwise, the intake plugging is suspected when the dead head matches the theoretical pump head (El Gindy et al. 2015; Agrawal et al. 2019). This study adopted a rate-derating factor to represent a dead head test. It is related to the deadhead test because rate derating can detect the change in the pump head at the shut-in point (zero flow) or the AOF (maximum flow rate).

Figure 10a and b shows the change in the ESP performance curve (ESP head curve) with increases according to the IPF variation by considering the single-phase and multiphase flows, respectively. It is perceived that the ESP performance curve shifted to the left side with an increase in the IPF, and AOF decreased by following similar trends. Besides, a steady head at the shut-in point (zero flow rate) implies that whenever the pump is experiencing an intake plugging issue at no flow condition, the maximum head will be maintained. Moreover, the rate derating based on the ESP operating point was recorded at each ESP performance curve obtained from different IPFs (Fig. 10c&d); the increases in the IPF have further heightened the percentage of the rate derating until the pump failed to deliver an additional head. These results concurred with other findings; for instance, the experimental test conducted on the plugged ESP has shown that as the solid deposition at the pump intake elevated, the

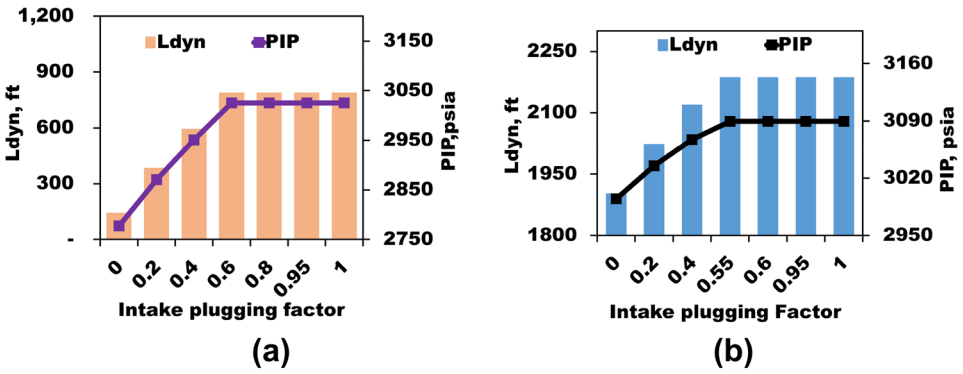

Fig. 9 Variation of pump intake pressure and annulus liquid level **a** Intake plugging effects in multiphase conditions (GOR = 2218 SCF/STB and water = 92.9%). **b** Intake plugging effects in single-phase conditions (GOR = 100 SCF/STB and water = 0)

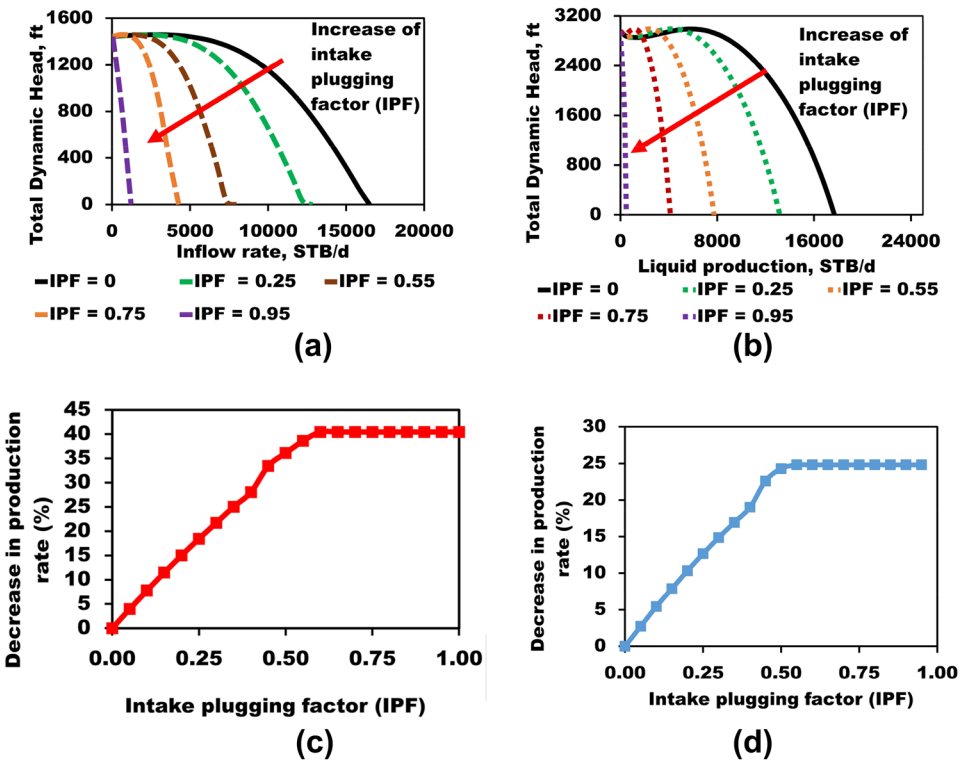

Fig. 10 Effect of the Intake plugging on the ESP performance **a** in a single-phase well (fixed GOR = 100 SCF/STB and water = 0). **b** A multiphase well (GOR = 2218 SCF/STB and water = 92.9%). A decrease in production rate (rate-derating percentage) **c** in a single-phase well (fixed GOR = 100 SCF/STB and water = 0). **d** A multiphase well (GOR = 2218 SCF/STB and water = 92.9%)

ESP performance curve forcedly moved to the left, modifying the pump operating point (Divine et al. 1993). Likewise, Agrawal et al. (2019) reported that nearly the complete plugging, the ESP pump is operating at its maximum head (which is a zero flow condition); this is the point the AOF is near to the shut-in point (zero flow rate), which is the same result observed when the IPF is 0.95.

Field example

This section featured some field examples from the reported technical paper, indicating how the downhole data is used to show the ESP plugging problem. This helps to understand how the mentioned methodology can be linked to ESP well monitoring.

Example 1 This example reflects the oil field example in the Flanagan oil field in Western Texas. Previously, the ESP ran smoothly except for the small spikes (Fig. 11, points A, B, and C). At the spike, the intake pressure increased from 200 to 300 psi; hence, different failures (e.g., gas breakout or fluid composition change) were suspected to be the cradle of that spike in the downhole data tides. After a while, a dramatic fluctuation was noticed from March 25, 2005, when PIP increased from 180 to 900 psi (Fig. 11, point D). Afterward, the ESP operating speed decreased from 55 Hz to approximately zero. The well troubleshooting confirmed the problem resulted from partial intake plugging (linked to the

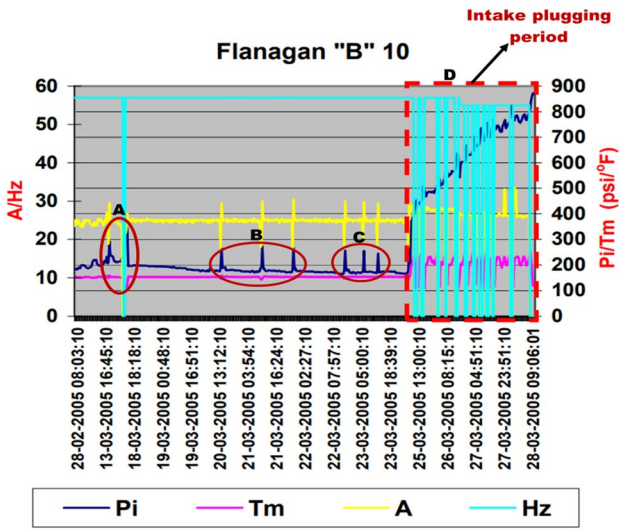

Fig. 11 Example 1: PIP variation during the intake plugging (Pi: Intake pressure, *Tm*: Motor temperature, A: Amperage, and *Hz*: ESP speed modified from Oyewole (2005)

IPF = over 0.5 in the proposed methodology), which reduced the intake fluid. Reduced fluid entering the pump increased the PIP recorded on March 25, 2005 (Fig. 11, point D). The drop in the ESP speed is a response to the lower volumetric rate (production rate). This example provided a way of interpreting the spike observed in the previous period (Fig. 11, Points A, B, and E). The PIP spike in that period arose from

the pump intake plugged momentarily, and less fluid entered the pump, causing a sudden increase in the PIP.

Example 2 Depicts the ESP oil well in the Midland (Texas) Permian Basin. As shown in Fig. 12, point a, the ESP was running smoothly; however, due to the ESP intake plugging, the abrupt increase of the pump intake pressure was recorded (Fig. 12, point b). Due to the decreased volumetric flow rate, the ESP speed suddenly fell from 55 Hz to approximately zero. Consequently, the intake plugging was suspected to be the root of the abnormal conditions, later confirmed in the oil well diagnosis, and found that the well exhibited a bacterial issue, which plugged the ESP intake point. The chemical treatment was conducted using a biocide, and removed the plugging material. As shown in Fig. 12, point c, ESP returns to its normal operating condition after treatment. The PIP dropped to the normal running point, which increased the ESP operating speed to the normal range, and other parameters operated consistently (Fig. 12, point d).

Conclusions and recommendations

This study presented the application of the intake plugging and rate-derating factor to evaluate the effects of cumulative intake plugging on the ESP operation using the nodal analysis. The quantitative standard for the normal and abnormal intake plugging factor (IPF) range was established based on the existing intake plugging field data. The analysis of the variation of the ESP-assisted well parameters (such as PIP, Ldyn, and q) over that range was conducted, and the following conclusions were obtained.

1. The intake plugging failure can be managed using nodal analysis by setting the IPF threshold operating range, which proactively monitors the new ESP well.
2. A predefined IPF threshold range and rate derating (dead head test) differentiates the intake plugging issue from other failures, allows quick interpretation of the downhole data, and facilitates rapid oil well diagnosis and treatment.
3. The developed approach does not require extensive computation; it uses nodal analysis software, which facilitates an evaluation of the ESP operating condition before and after installation if solid deposition is suspected in the production well.

The work is novel in presenting a normal operating range of several intake plugging conditions: Normal operating range (the plugging conditions that permit the ESP operating rate higher than the original natural oil well condition) and provides a proactive monitoring plan before and after ESP deployment based on the ESP natural well conditions in contrast to the existing approach only provides the retrospective condition of the ESP failure.

The limitation of the work is that the intake plugging factor relies on the quantitative assumption of the area of the intake screen plugged with solids, and these values need to be calibrated against the field condition. Therefore, the intake plugging parameter was not previously considered, which limits data availability.

We recommend applying the proposed approach where the solid deposition is present. Also, in the future, the intake plugging factor should be integrated as an additional parameter of the intelligent oil well control station to map the percentage of the pump intake area plugged with solids and linked to the ESP operating parameters, which provide a

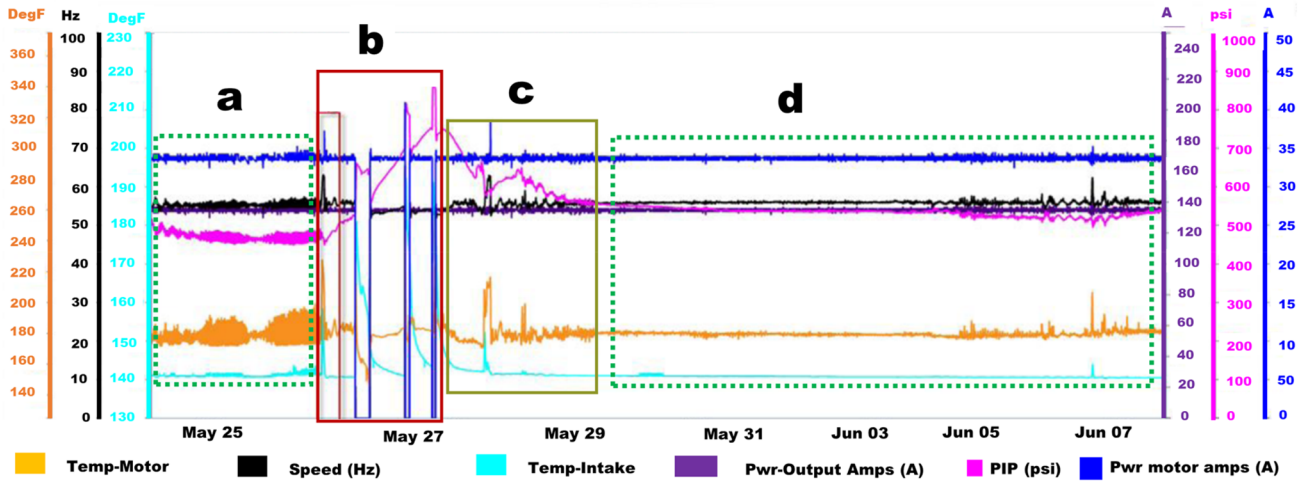

Fig. 12 Example 2: Pump intake pressure (PIP) variation during the intake plugging modified from Adesanwo et al. (2016)

future direction of the monitoring of a cumulative plugging in the ESP well.

Acknowledgements This work was supported by the Development of Intelligential Diagnosis, Abandonment Process and Management Technology for Decrepit Oil and Gas Wells of the Korea Institute of Energy Technology Evaluation and Planning (KETEP), granted financial resources from the Ministry of Trade, Industry & Energy, and Republic of Korea (No. 20216110100010).

Funding This work was supported by the "Development of Intelligential Diagnosis, Abandonment Process and Management Technology for Decrepit Oil and Gas Wells" of the Korea Institute of Energy Technology Evaluation and Planning(KETEP) granted financial resource from the Ministry of Trade, Industry & Energy, Republic of Korea (No. 20216110100010).

Declarations

Conflict of interest All the authors have approved the manuscript and agreed with submission to your esteemed journal. There are no conflicts of interest to declare.

References

Abdelazim A, Abu El Ela M, El-Banbi A, Sayyouh H (2022) Successful approach to mitigate the asphaltenes precipitation problems in ESP oil wells. J Pet Explor Prod Technol 12(3):725–741. https://doi.org/10.1007/s13202-021-01335-7

Adesanwo M, Denney T, Lazarus S, Bello O (2016) Prescriptive-based decision support system for online real-time electrical submersible pump operations management. In: SPE Intelligent Energy International Conference and Exhibition (SPE-181013-MS). https://doi.org/10.2118/181013-MS

Adesanwo M, Oladele B, Olumide O, Obehi E, Sherif S, Eyituoyo B (2017) Advanced analytics for data-driven decision making in electrical submersible pump operations management. In: SPE Nigeria Annual International Conference and Exhibition (SPE-189119-MS). https://doi.org/10.2118/189119-MS

Agrawal N, Chapman T, Baid R, Singh RK, Shrivastava S, Kushwaha MK, Kolay J, Ghosh P, Das J, Khare S, Kumar P, Aggarwal S (2019) ESP performance monitoring and diagnostics for production optimization in polymer flooding: a case study of Mangala field. In: SPE Oil and Gas India Conference and Exhibition (D022S028R002). https://doi.org/10.2118/194656-MS

Alcock DN (1981) Production operation of submersible pumps with closed-loop adjustable speed control. IEEE T Ind Appl 5:481–489. https://doi.org/10.1109/TIA.1981.4503986

Alizadeh A, Nakhli H, Kharrat R, Ghazanfari MH (2011) An experimental investigation of asphaltene precipitation during natural production of heavy and light oil reservoirs: the role of pressure and temperature. Pet Sci Technol 29(10):1054–1065. https://doi.org/10.1080/10916460903530531

Awaid A, Al-Muqbali H, Al-Bimani A, Al-Yazeedi Z, Al-Sukaity H, Al-Harthy K, Baillie A (2014) ESP well surveillance using pattern recognition analysis, oil wells, petroleum development Oman. In: SPE—International Petroleum Technology Conference 2014 (IPTC 17413-MS). https://doi.org/10.3997/2214-4609-pdb.395.iptc-17413-MS

Babu DK, Odeh AS (1989) Productivity of a horizontal well. SPE Reserv 4(04):417–421. https://doi.org/10.2118/18298-PA

Beggs DH, Brill JP (1973) A study of two-phase flow in inclined pipes. J Pet Technol 25(05):607–617. https://doi.org/10.2118/4007-PA

Bermudez F, Carvajal GA, Moricca G, Dhar J, Md Adam F, Al-Jasmi A, Goel HK, Nasr H (2014) Fuzzy logic application to monitor and predict unexpected behavior in electric submersible pumps (Part of the KwIDF Project). In: SPE Intelligent Energy International 2014 (SPE 167820-MS). https://doi.org/10.2118/167820-MS

Bruijnen PM (2016) Nodal analysis by use of ESP intake and discharge pressure gauges. SPE Prod Oper 31(01):76–84. https://doi.org/10.2118/178433-PA

Chouparova E, Lanzirotti A, Feng H, Jones KW, Marinkovic N, Whitson C, Philp P (2004) Characterization of petroleum deposits formed in a producing well by synchrotron radiation-based microanalyses. Energy Fuels 18(4):1199–1212. https://doi.org/10.1021/ef030108a

Correra S, Iovane M, Pinneri S (2016) Role of electrical submerged pumps in enabling asphaltene-stabilized emulsions. Energy Fuels 30(5):3622–3629. https://doi.org/10.1021/acs.energyfuels.5b02083

Denney D (2000) Asphaltene deposition in electrical-submersible-pump applications. J Pet Technol 52(05):35–36. https://doi.org/10.2118/0599-0035-JPT

Dholkawala ZFF, Daniel S, Billingsley B (2012) From operations to desktop analysis to field implementation: Well and ESP optimization for production enhancement in the Cliff head field. SPE Prod Oper 27(01):52–66. https://doi.org/10.2118/128003-PA

Divine DL, Lannom RW, Johnson RA (1993) Determining pump wear and remaining life from electric submersible pump test curves. SPE Prod Facil 8(03):217–221. https://doi.org/10.2118/22399-PA

Dowling M, Lemus A (2023) ESPs in high productivity wells and use of pressure derivatives to understand behavior. In: SPE Gulf Coast Section—Electric Submersible Pumps Symposium (SPE-214744-MS). https://doi.org/10.2118/214744-MS.

Fakher S, Khlaifat A, Hossain ME, Nameer H (2021) Rigorous review of electrical submersible pump failure mechanisms and their mitigation measures. J Pet Explor Prod Technol 11(10):3799–3814. https://doi.org/10.1007/s13202-021-01271-6

Gindy M, Abdelmotaal H, Botros K, Ginawi I, Sayed E, Edris T (2015) Monitoring & surveillance improve ESP operation and reduce workover frequency. In: SPE—Abu Dhabi International Petroleum Exhibition and Conference (SPE-177926-MS). https://doi.org/10.2118/177926-MS

Hagedorn AR, Brown KE (1965) Experimental study of pressure gradients occurring during continuous two-phase flow in small-diameter vertical conduits. J Pet Technol 17(04):475–484. https://doi.org/10.2118/940-PA

Iranzi J, Son H, Lee Y, Wang J (2022) A nodal analysis based monitoring of an electric submersible pump operation in multiphase flow. Appl Sci 12(6):2825. https://doi.org/10.3390/app12062825

Lea JF, Nickens HV (2004) Solving gas-well liquid-loading problems. J Pet Technol 56(04):30–36. https://doi.org/10.2118/72092-JPT

Manshad AK, Dastgerdi ME, Ali JA, Mafakheri N, Keshavarz A, Iglauer S, Mohammadi AH (2019) Economic and productivity

evaluation of different horizontal drilling scenarios: Middle East oil fields as case study. J Pet Explor Prod Technol 9(4):2449–2460. https://doi.org/10.1007/s13202-019-0687-9

Mohammadzadeh O, Taylor SD, Eskin D, Ratulowski J (2018) Experimental investigation of asphaltene-induced formation damage caused by pressure depletion of live reservoir fluids in porous media. SPE J 24(01):1–20. https://doi.org/10.2118/187053-PA

Oyewole P (2005) Application of real-time ESP data processing and interpretation in Permian basin "Brownfield" operation. In: International Petroleum Technology Conference (IPTC-10927-MS). https://doi.org/10.2523/IPTC-10927-MS

Pagan EV, Waltrich PJ (2016) A simplified model to predict transient liquid loading in gas wells. J Nat Gas Sci Eng 35:372–381. https://doi.org/10.1016/j.jngse.2016.08.059

Powers ML (1987) Effects of speed variation on the performance and longevity of electric submersible pumps. SPE Prod Eng 2(01):15–24. https://doi.org/10.2118/14349-PA

Ramones M, Rachid R, Flor D, Gutierrez L, Milne A (2015) Removal of organic and inorganic scale from electric submersible pumps. In: SPE Artificial Lift Conference—Latin America and Caribbean (SPE-173928-MS). https://doi.org/10.2118/173928-MS

Takacs G (2011) How to improve poor system efficiencies of ESP installations controlled by surface chokes. J Pet Explor Prod Technol 1(2–4):89–97. https://doi.org/10.1007/s13202-011-0011-9

Takacs G (2018) Chapter 3 - Electrical submersible pump components and their operational features. In: Electrical Submersible Pumps Manual, 2nd Edn, Gulf Professional Publishing, pp. 55–152. https://doi.org/10.1016/B978-0-12-814570-8.00003-9

Vazirian MM, Charpentier TVJ, de Oliveira PM, Neville A (2016) Surface inorganic scale formation in oil and gas industry: as adhesion and deposition processes. J Pet Sci Eng 137:22–32. https://doi.org/10.1016/j.petrol.2015.11.005

Wilson BL, Liu JC (1985) Electrical submersible pump performance using variable speed drives. In: SPE Production Operations Symposium (SPE-13805-MS). https://doi.org/10.2118/13805-MS

Xian W, Wenyu L, Yan P (2014) A new method of BHP measurement in ESP deadhead test. In: Offshore Technology Conference-Asia (OTC-24701-MS). https://doi.org/10.4043/24701-MS

Yadua AU, Lawal KA, Okoh OM, Ovuru MI, Eyitayo SI, Matemilola S, Obi CC (2020) Stability and stable production limit of an oil production well. J Pet Explor Prod Technol 10(8):3673–3687. https://doi.org/10.1007/s13202-020-00985-3

Zendehboudi S, Shafiei A, Bahadori A, James LA, Elkamel A, Lohi A (2014) Asphaltene precipitation and deposition in oil reservoirs—technical aspects, experimental and hybrid neural network predictive tools. Chem Eng Res and Des 92(5):857–875. https://doi.org/10.1016/j.cherd.2013.08.001